RSC Advances

PAPER

View Article Online
View Journal | View Issue



Cite this: *RSC Adv.*, 2019, **9**, 29070

# Development of improved dual-diazonium reagents for faster crosslinking of tobacco mosaic virus to form hydrogels†

Dejun Ma, ‡[b] Zhuoyue Chen,‡[a] Long Yi *[a] and Zhen Xi*[bc]

Received 21st July 2019
Accepted 9th September 2019

DOI: 10.1039/c9ra05630k

rsc.li/rsc-advances

New bench-stable reagents with two diazonium sites were designed and synthesized for protein crosslinking. Because of the faster diazonium-tyrosine coupling reaction, hydrogels from the crosslinking of tobacco mosaic virus and the reagent **DDA-3** could be prepared within 1 min at room temperature. Furthermore, hydrogels with the introduction of disulfide bonds *via* **DDA-4** could be chemically degraded by dithiothreitol. Our results provided a facile approach for the direct construction of virus-based hydrogels.

## Introduction

Hydrogels are widely used as biomedical materials in manufacturing cell culture matrices,[1] tissue engineering scaffolds,[2] drug delivery systems[3] and wound dressings[4] due to their unique properties, such as water retention capacity, softness, controllability and biocompatibility.[5] One of the main approaches for preparing hydrogels is the chemical crosslinking of hydrophilic polymers (natural or synthetic) to provide desirable mechanical and chemical properties.[6] As natural hydrophilic polymers, plant viruses like tobacco mosaic virus (TMV, 300 nm × 18 nm) exhibit a nanoscale size and abundant amino acid residues on their surface of capsid proteins, which facilitate facile chemical reactions to produce nanomaterials with multiple functions.[7] Furthermore, plant viruses could be largely produced in gram-scale quantities and are also considered much safer to mammals than human-associated viruses like adenovirus and lentivirus in drug delivery and tissue engineering.[8] Hence, using of plant viruses as building blocks to assemble virus-based hydrogels is attractive in biomedical applications.[9]

Recently, there are mainly two approaches to utilizing plant viruses to construct hydrogels. Firstly, mixture of TMV with hydrogels alters their properties. As reported, the incorporation of TMV into the porous alginate hydrogels greatly reduced the immunogenicity in mice, and the covalent incorporation of tobacco mosaic virus into poly (ethylene glycol) diacrylate hydrogels increased the stiffness.[10] Secondly, the hydrogels are directly made through chemically crosslinking TMV virus matrix, which was rarely explored. In our previous work, a TMV-based hydrogel was prepared by crosslinking TMV with a dual-diazonium reagent **DDA-1** (Scheme 1).[11] However, the virus-based hydrogels should be made within at least 30 min at 37 °C due to the relatively low diazonium-tyrosine (Tyr) coupling reaction[12] between **DDA-1** and Tyr residues.

In this work, we designed and synthesized three new dual-diazonium reagents (**DDA-2**, **DDA-3**, **DDA-4**) to investigate the effects of substituents (CO, PO, $SO_2$) on the crosslinking efficiency and gelation conditions. To our delight, **DDA-3**/**DDA-4** could quickly crosslink TMV matrix as hydrogels within 1 min at room temperature. Moreover, the **DDA-4**-based hydrogel could

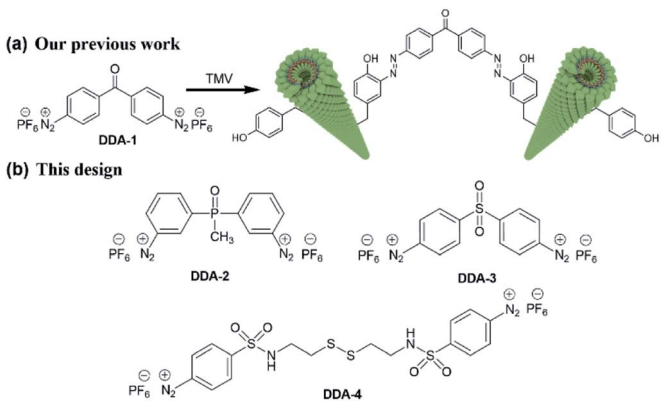


Scheme 1 (a) Schematic illustration for crosslinking *via* TMV and **DDA-1** in our previous work; (b) the chemical structure of new dual-diazonium reagents (**DDA-2**, **DDA-3** and **DDA-4**).

[a]*State Key Laboratory of Organic-Inorganic Composites, Beijing University of Chemical Technology, Beijing 100029, China. E-mail: yilong@mail.buct.edu.cn*

[b]*State Key Laboratory of Elemento-Organic Chemistry, Department of Chemical Biology, National Pesticide Engineering Research Center (Tianjin), Nankai University, Tianjin, 300071, China. E-mail: zhenxi@nankai.edu.cn; Tel: +86 22 23504782*

[c]*Collaborative Innovation Center of Chemical Science and Engineering, Nankai University, Tianjin, 300071, China*

† Electronic supplementary information (ESI) available. See DOI: 10.1039/c9ra05630k

‡ The authors contribute equally to the work.

be efficiently degraded with reducing chemicals like dithiothreitol (DTT), which enhanced the biocompatibility and biodegradability of such hydrogel.

## Results and discussion

As shown in Scheme 2, **DDA-2** was obtained by nitration, reduction, diazotization and hexafluorophosphoric acid precipitation from the inexpensive methyl biphenyl phosphine oxide. The final product **DDA-2** (white solid) was obtained after mixing **2** with the concentrated HCl, $NaNO_2$ and $HPF_6$ in one-pot. **DDA-3** (light yellow solid) could be prepared from 4,4′-diaminodiphenyl sulfone in one-pot synthesis. For **DDA-4**, cystamine was firstly reacted with 4-acetamidobenzenesulfonyl chloride to provide **3**, which was then hydrolysed with the concentrated HCl to give **4**. After treatment of the concentrated HCl, $NaNO_2$ and $HPF_6$ in one-pot, a yellow solid **DDA-4** was obtained with good yield.

These dual-diazonium reagents (**DDA-2**, **DDA-3** and **DDA-4**) were well characterized by $^1$H NMR, $^{13}$C NMR, $^{31}$P NMR (see the ESI†). Compared with the chemical shift of **2** in $^1$H NMR (less than 8 ppm), the high chemical shift (9.19, 8.86, 8.63 and 8.17 ppm) of **DDA-2** implied the existence of a positively charged diazonium moiety. Affected by phosphorus, the methyl group in **DDA-2** was split into two peaks in $^1$H NMR and $^{13}$C NMR. The $^{31}$P NMR implied the existence of two kinds of phosphorus, in which the seven peaks were the result of the coupling of six fluorine nucleuses in hexafluorophosphate. Since the dual-diazonium salt was not successfully characterized by mass spectrum, we tried to react **DDA-2** with 4,4′-methylenediphenol to get **5**. The structure of **5** was clearly confirmed by $^1$H NMR, $^{13}$C NMR spectra and high-resolution mass spectra (HRMS), which was indirectly verified that the obtained diazonium salt was **DDA-2** (see the ESI†). As for **DDA-3** and **DDA-4**, the high chemical shift values in $^1$H NMR compared to their aromatic amine feedstock also implied the existence of positively charged diazo moieties. All dual-diazonium hexafluorophosphates were bench-stable and could be stored in the refrigerator (−20 °C) for at least two months.

We firstly studied the reaction of **DDA-2** or **DDA-3** with Tyr using the UV-Vis spectrophotometry (Fig. 1). The time-dependent absorption changes at 400 nm implied the formation of azo bonds[11,12] and enabled us to follow the reaction kinetics conveniently. When the dual-diazonium reagent and Tyr were mixed under pseudo-first-order conditions, the absorption peak at 400 nm was monitored with time. The pseudo-first-order rate $k_{obs}$ was determined by fitting the data with a single exponential function. The linear fitting between $k_{obs}$ and Tyr concentrations gave the reaction rate ($k_2$). **DDA-2** showed much smaller $k_2$ (18.39 $M^{-1}$ $s^{-1}$) than that of **DDA-3** (71.19 $M^{-1}$ $s^{-1}$), implying that the substitution of CO group with $SO_2$ group greatly enhanced the reaction rate (Fig. 1, S1 and S2†). Substituents linked to aromatic cycles could affect the reactivity of diazonium with Tyr due to conjugate and other effects. Herein, the Hammett equation was further used to study the relationship between the *para* and *meta* substituents

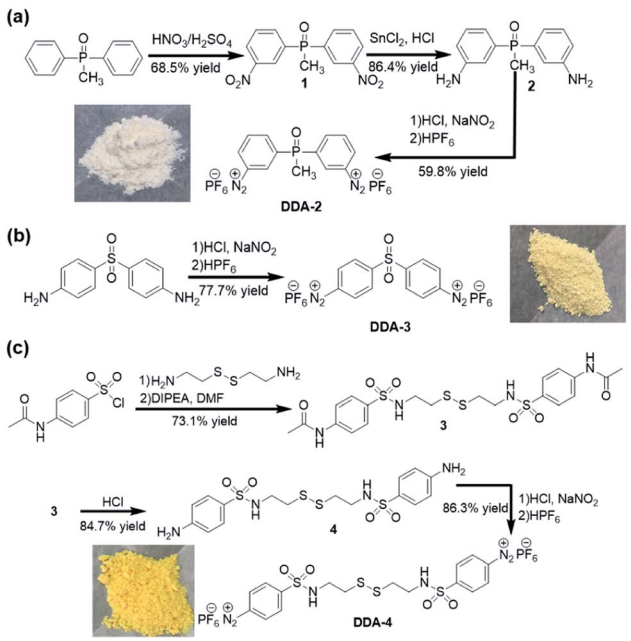


Scheme 2 The synthesis route for the dual-diazonium reagents **DDA-2** (a), **DDA-3** (b) and **DDA-4** (c).

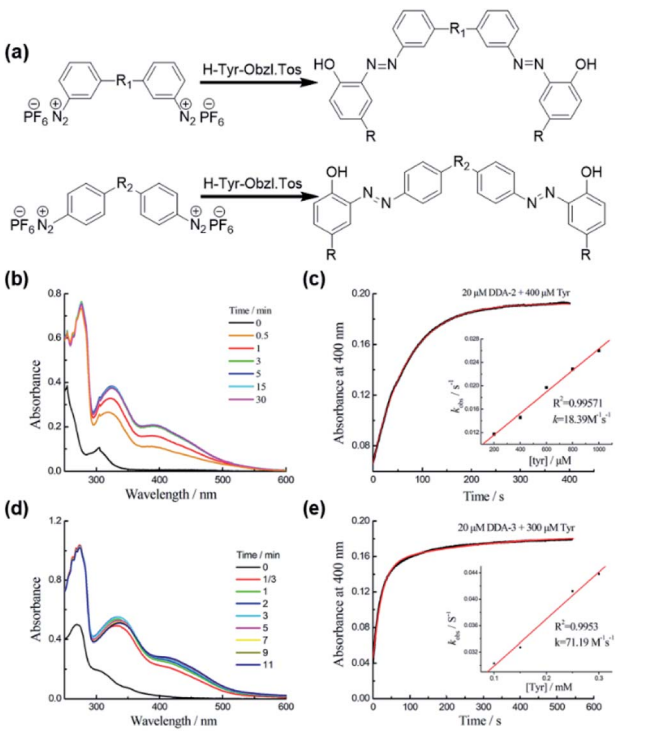


Fig. 1 Kinetic assay of dual-diazonium reagents with Tyr. (a) Azo-coupling reaction of diazonium reagent with Tyr, $R_1 = POCH_3$ (**DDA-2**), $R_2 = SO_2$ (**DDA-3**); (b) time-dependent UV-Vis absorbance spectra of **DDA-2** (20 μM) with Tyr (400 μM); (c) time-dependent absorbance at 400 nm of **DDA-2** with Tyr; (d) time-dependent UV-Vis absorbance spectra of **DDA-3** (20 μM) with Tyr (300 μM); (e) time-dependent absorbance at 400 nm of **DDA-3** with Tyr. The rate constants of the azo-coupling reactions are indicated in the inset.

of benzene derivatives and the reaction rate. In this work, the Hammett parameter $\sigma$[13] was obtained by using two kinds of similar structural substituents (Fig. S3†).[14] By comparing the reactivity of the three diazonium salts, we found that the crosslinking rate of the diazonium cations and Tyr was higher with increasing electron withdrawing of the substituent: **DDA-3** > **DDA-1** > **DDA-2**. Remarkably, the slope of the linear fit was positive, demonstrating that the electron-withdrawing substituents accelerated the reaction, which was consistent with the kinetic results. This study might help us to construct more efficient multi-diazonium reagents in the future.

To compare the efficiency of dual-diazonium reagents (**DDA-1**, **DDA-2**, **DDA-3**) in protein labelling, we firstly used these reagents to crosslink the capsid proteins from tobacco mosaic virus (TMV CP) at 25 °C. The SDS-PAGE assay revealed that **DDA-3** had higher crosslinking efficiency than that of **DDA-1** and **DDA-2** at room temperature. When the concentration of **DDA-3** reached at least 1.25 mM, the percentage of crosslinked capsid proteins could be more than 85%. At such concentration, **DDA-1** and **DDA-2** could just achieve 30–50% protein crosslinking (Fig. 2).

Subsequently, we used these reagents to crosslink TMV virus at 25 °C and 37 °C. Based on SDS-PAGE analysis, we also found that the crosslinking efficiency of **DDA-3** at 37 °C were slightly higher than that at 25 °C while the crosslinking efficiency of **DDA-1** at 25 °C was significantly lower than that at 37 °C (Fig. S4–S6†). Furthermore, time-dependent crosslinking of TMV also suggested that the reaction could finish within 10 min for **DDA-3** (Fig. S7†) and not finish until 60 min for **DDA-1** (Fig. S8†) at 25 °C. These results clearly demonstrated that the substitution of CO group with $SO_2$ group in the linker reagent greatly enhanced the speed and efficiency of protein crosslinking and TMV crosslinking at room temperature.

Encouraging with the above results, we then employed these reagents to crosslink TMV virus matrix to construct hydrogels. We firstly performed the time- and dose-dependent gelation tests. The results showed that 10 mM **DDA-3** could completely solidify TMV matrix (2.5 mg $mL^{-1}$) in 1 min at 25 °C. While for **DDA-2**, the complete gelation should cost at least 15 min under similar conditions (Fig. S9†). Therefore, we further used **DDA-3** in following studies. The dose-dependent tests also suggested that 1.25 mM **DDA-3** and 1.25 mg $mL^{-1}$ TMV matrix were the minimum concentration for gelation within 30 min (Fig. 3, S10 and S11†). The high concentration of crosslinker and TMV matrix like 10 mM **DDA-3** and 5 mg $mL^{-1}$ TMV matrix also provided the high solidification. These results implied that improved dual-diazonium reagents could be used for faster crosslinking of tobacco mosaic virus as hydrogels, which further simplify the gelation method.

To further probe the crosslinking efficiency, we subsequently determined the rheological characters of the hydrogels formed by TMV and **DDA-2** or **DDA-3** from the solution phase to gel phase. As shown in Fig. 4a, the viscosity of both hydrogels started to increase after 100 s, while the hydrogel with **DDA-3** showed higher viscosity (about 2.5-fold) than that with **DDA-2**, implying that **DDA-3** had the higher gelation efficiency. Both the hydrogels were solidified after 400 s. Moreover, we also analysed the storage modulus of TMV hydrogels (Fig. 4b) and found that the hydrogel based on **DDA-3** had much faster gelation speed with a relatively higher storage modulus than that based on **DDA-2**. These results indicate that the improved reagent **DDA-3** could be used for faster crosslinking of TMV as hydrogels than **DDA-2**.

We further used scanning electron microscope (SEM) to analyze the structure of TMV hydrogels from 10 mM **DDA-2** or **DDA-3** and 5 mg $mL^{-1}$ TMV. SEM results showed multiple virus

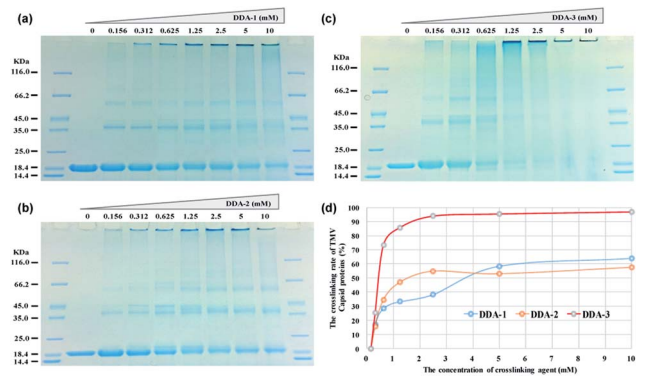


Fig. 2 The crosslinking of capsid proteins from tobacco mosaic virus with three crosslinking reagents. The dual-diazonium reagent (**DDA-1**, **DDA-2** or **DDA-3**) was firstly dissolved in DMSO and then diluted to a gradient concentration (100, 50, 25, 12.5, 6.25, 3.12, 1.56, mM). The reaction was performed by mixing 9 μL TMV capsid proteins (2 μg $\mu L^{-1}$) and 1 μL dual-diazonium reagent with various concentrations. The reaction was incubated at 25 °C for 30 min. After reaction, 10 μL sample for each treatment was directly used for 12% SDS-PAGE assay.

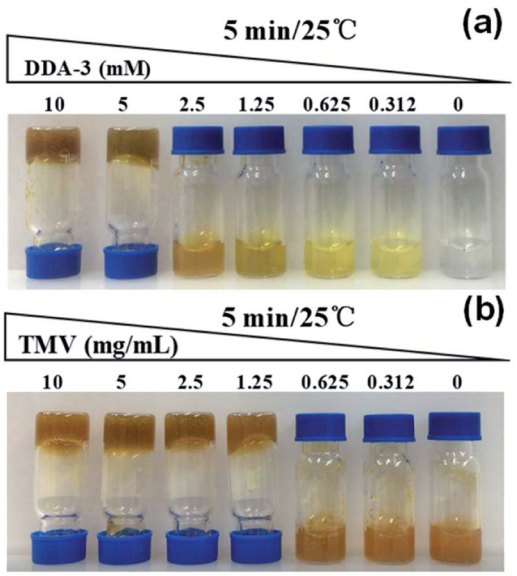


Fig. 3 Dose-dependent TMV gelation. (a) The effect of the concentration of **DDA-3** on TMV gelation. The final concentration of **DDA-3** was varying from 0–10 mM and the concentration of TMV matrix was 2.5 mg $mL^{-1}$. (b) The effect of the concentration of TMV matrix on TMV gelation. The final concentration of TMV matrix was varying from 0–10 mg $mL^{-1}$ and the concentration of **DDA-3** was 10 mM. The gelation time was kept within 5 min at room temperature.

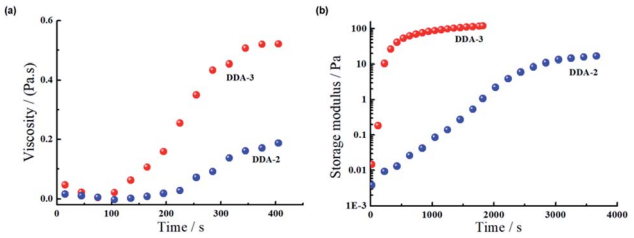


Fig. 4 Rheological characters of TMV hydrogels. (a) The viscosity of TMV hydrogels with **DDA-2** or **DDA-3** was measured within 400 s at 25 °C at a shear rate of 1 $s^{-1}$. (b) The storage modulus of TMV hydrogels with **DDA-2** or **DDA-3** was measured within 4000 s at 25 °C. The scanning strain value and the oscillation frequency were set as 1% and 0.1 Hz, respectively.

rods in **DDA-2** constructed hydrogel was crosslinked to form the 3D net structure, while a large number of sheets and less net structure were observed in **DDA-3** constructed hydrogel (Fig. 5).

Considering the importance of biocompatibility and degradability of hydrogels in applications, we also synthesized **DDA-4** through introducing a disulfide bond on the basis of **DDA-3.** The **DDA-4** has similar ability as **DDA-3** for TMV gelation (Fig. S9†). We then used the TMV hydrogels with **DDA-4** to make the capital "BUCT" and "NKU" in the dish (Fig. 6), and determined whether the hydrogels could be degraded by reducing chemicals like DTT. After the gelation, we immersed the gel in the DTT solution (500 mM) and observed the degradation of the gel within 8 h, suggesting the disulfide bond was gradually cleaved by DTT (Fig. 6 and S12†). On the contrary, the same hydrogel in the dish was not affected when no DTT was added. We believe that this kind of disulfide bond-based hydrogel could be disrupted by reducing

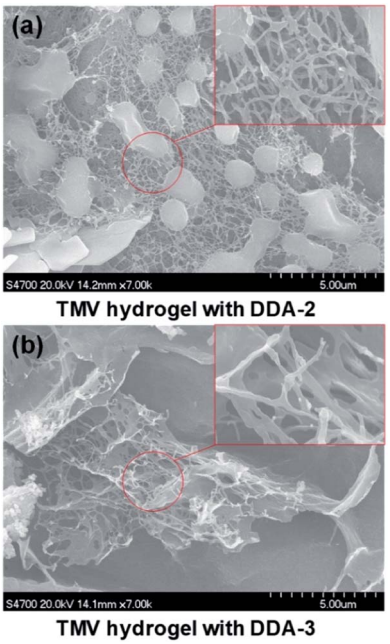


Fig. 5 Characterization of the TMV hydrogel with **DDA-2** (a) and **DDA-3** (b) by SEM. Scale bar, 500 μm for full view and 500 nm for the red rectangular box.

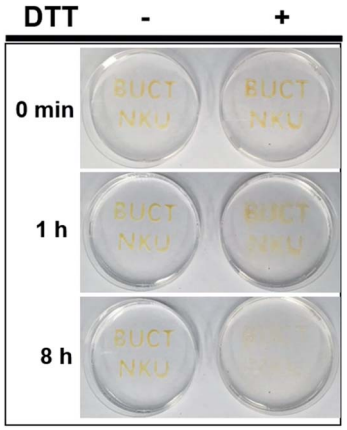


Fig. 6 TMV hydrogel degradation with dithiothreitol (DTT). The capital "BUCT" and "NKU" were made from TMV hydrogel crosslinked with **DDA-4** on the Petri dish. After gelation, the TMV hydrogel was immersed with 20 mL DTT (500 mM) or 20 mL deionized water. The gel degradation was imaged at different time (0 min, 1 h, 8 h).

molecules *in vivo*, which might add its biocompatibility for chemically controlled disassembly.[15]

## Conclusions

To improve the reaction rate and gelation efficiency, we developed new bench-stable reagents with different substituents (CO, PO, $SO_2$) between two diazonium sites. Through comparing the reaction rate constant and protein crosslinking efficiency, we found that **DDA-3** greatly improved the crosslinking efficiency and also shortened the gelation time even at room temperate, which was a great improvement compared with **DDA-1.**[11] The SDS-PAGE and SEM characterizations also confirmed the virus crosslinking *via* the dual-diazonium reagents. Furthermore, hydrogels with the introduction of disulfide bonds *via* **DDA-4** could be chemically degraded by biocompatible reducing molecules. We propose that the new dual-diazonium reagents may provide a general approach to preparing diverse functional hydrogels from other biocompatible viruses for future biomedical applications.

## Experimental

### General

All chemicals and solvents used for synthesis were purchased from commercial suppliers and applied directly in the experiments without further purification. The progress of the reaction was monitored by TLC on pre-coated silica plates (Merck 60F-254, 250 μm in thickness), and spots were visualized by UV light (254 nm). Merck silica gel (100–200 mesh) was used for general column chromatography purification. $^1$H NMR and $^{13}$C NMR spectra were recorded on a Bruker 400 spectrometer. Chemical shifts are reported in parts per million relative to internal standard tetramethylsilane ($Si(CH_3)_4 = 0.00$ ppm) or residual solvent peaks (DMSO-$d_6 = 2.50$ ppm, $^1$H; 39.52 ppm, $^{13}$C). $^1$H NMR coupling constants ($J$) are reported in hertz (Hz), and multiplicity is indicated as the

following: s (singlet), d (doublet), t (triplet), q (quartet), td (triplet doublet), dd (doublet of doublets), m (multiple). High-resolution mass spectra (HRMS) were obtained on an Agilent 6540 UHD Accurate-Mass Q-TOFLC/MS. The UV-Visible spectra were recorded on a UV-6000 UV-VIS-NIR-spectrophotometer (METASH, China).

### Synthesis of DDA-2

Methyl diphenyl phosphine oxide (4.89 g, 22.6 mmol) was dissolved in concentrated sulfuric acid (20 mL), and stirred under ice-cooling to dissolve the solid. A mixture of concentrated sulfuric acid (20 mL) and concentrated nitric acid (20 mL) was slowly added dropwise with a dropper. After the addition was completed, the ice bath was removed and the mixture was stirred at room temperature overnight. The reaction was monitored by TLC ($CH_2Cl_2$ : MeOH = 19 : 1). The reaction mixture was poured into ice water and then the precipitated solid were collected by filtration. After being washed with saturated aqueous $NaHCO_3$ until neutral pH, the product was recrystallized with absolute ethanol, yielding a light-yellow solid of **1** (4.74 g, 68.5%). $^1$H NMR (400 MHz, DMSO-$d_6$) $\delta$ 8.61 (d, $J$ = 12.0 Hz, 2H), 8.41 (d, $J$ = 8.1 Hz, 2H), 8.29 (dd, 2H), 7.85 (td, $J$ = 7.9, 2.6 Hz, 2H), 2.31 (d, $J$ = 14.1 Hz, 3H); $^{13}$C NMR (101 MHz, DMSO-$d_6$) $\delta$ 148.0, 147.8, 137.0, 136.7, 136.6, 136.0, 130.8, 130.7, 126.7, 126.7, 125.0, 124.9, 15.6, 14.9.

Tin II chloride (14.48 g, 64.2 mmol) was dissolved in 40 mL concentrated HCl. **1** (3.11 g, 10.1 mmol) was added portionwise with stirring and the reaction mixture was refluxed at 80 °C for 2 h. After the mixture had cooled to room temperature, the pH of the mixture was adjusted to 9–10 by the saturated solution of NaOH at 0 °C. The mixture was extracted with EtOAc. The organic phase was washed by brine and dried over anhydrous $Na_2SO_4$. After removing the solvent under reduced pressure, the product was purified by silica gel column chromatography to give **2** (2.15 g, 86.4%). $^1$H NMR (400 MHz, DMSO-$d_6$) $\delta$ 7.11 (td, $J$ = 7.7, 3.6 Hz, 2H), 6.89 (d, $J$ = 13.1 Hz, 2H), 6.78 (dd, $J$ = 11.1, 7.6 Hz, 2H), 6.67 (d, $J$ = 7.9 Hz, 2H), 5.31 (s, 4H), 1.81 (d, $J$ = 13.1 Hz, 3H); $^{13}$C NMR (101 MHz, DMSO-$d_6$) $\delta$ 148.8, 148.6, 136.2, 135.2, 129.1, 128.9, 117.1, 117.0, 116.4, 116.4, 115.2, 115.1, 16.4, 15.6; $^{31}$P NMR (162 MHz, DMSO-$d_6$) $\delta$ 28.63 (s).

**2** (998 mg, 4.0 mmol) was dissolved in 30 mL cold concentrated HCl and cooled down to 0 °C. The water solution of $NaNO_2$ (1.82 g, 26.4 mmol) was slowly added to the mixture at 0 °C. After reaction for 30 min, 4 mL 60% $HPF_6$ was added and the mixture was stirred for 1 h. The product was collected by filtration and washed by ice-cold water, yielding a creamy-white solid of **DDA-2** (1.34 g, 59.8%). $^1$H NMR (400 MHz, DMSO-$d_6$) $\delta$ 9.19 (d, $J$ = 11.5 Hz, 2H), 8.86 (d, $J$ = 8.2 Hz, 2H), 8.63 (t, 2H), 8.17 (t, $J$ = 7.6 Hz, 2H), 2.36 (d, $J$ = 14.2 Hz, 3H); $^{13}$C NMR (101 MHz, DMSO-$d_6$) $\delta$ 141.7, 141.6, 137.3, 136.4, 135.9, 135.1, 135.0, 132.0, 131.9, 118.0, 117.8, 15.5, 14.8; $^{31}$P NMR (162 MHz, DMSO-$d_6$) $\delta$ 26.52 (s), −144.20 (h, $J_{P\text{-}F}$ = 711.3 Hz).

### Synthesis of DDA-3

4,4′-Diaminodiphenyl sulfone (1.16 g, 4.6 mmol) was dissolved in 20 mL concentrated HCl and 40 mL $H_2O$ and cooled down to 0 °C. The water solution of $NaNO_2$ (2.07 g, 29.6 mmol) was slowly added to the mixture at 0 °C. After reaction for 1 h, 4 mL 60% $HPF_6$ was added and the mixture was stirred for 1 h. The product was collected by filtration and washed with methanol and dichloromethane, yielding a yellow solid of **DDA-3** (2.01 g, 77.7%). $^1$H NMR (400 MHz, DMSO-$d_6$) $\delta$ 8.94 (d, $J$ = 8.8 Hz, 4H), 8.65 (d, $J$ = 8.8 Hz, 4H); $^{13}$C NMR (101 MHz, DMSO-$d_6$) $\delta$ 147.6, 134.3, 130.6, 122.9; $^{31}$P NMR (162 MHz, DMSO-$d_6$) $\delta$ −144.19 (h, $J_{P\text{-}F}$ = 711.3 Hz).

### Synthesis of DDA-4

Cystamine dihydrochloride (0.99 g, 4.4 mmol) and 4-acetamidobenzenesulfonyl chloride (2.48 g, 10.6 mmol) was dissolved in 10 mL DMF. The mixture was stirred at 0 °C; DIPEA (3.4 mL, 20.0 mmol) was added into 10 mL DMF and add in batches with a syringe in portions at 0 °C. The mixture was stirred at room temperature overnight. The solvent was evaporated under reduced pressure and the crude was diluted with 50 mL dichloromethane. The product was collected by filtration and washed with dichloromethane to give **3** (1.76 g, 73.1%). $^1$H NMR (400 MHz, DMSO-$d_6$) $\delta$ 10.32 (s, 1H), 7.78–7.67 (m, 2H), 2.98 (q, $J$ = 13.1, 6.5 Hz, 1H), 2.66 (t, $J$ = 6.9 Hz, 1H), 2.08 (s, 1H); $^{13}$C NMR (101 MHz, DMSO-$d_6$) $\delta$ 169.0, 142.8, 133.9, 127.7, 118.7, 41.7, 37.0, 24.1.

**3** (1.16 g, 2.1 mmol) was dissolved in 40 mL concentrated HCl, and the mixture was stirred at 60 °C for 4 h. Then it was collected by filtration and the saturated solution of $NaHCO_3$ was added until pH 7–8. Next, the mixture was extracted with EtOAc, and the combined organic extracts were washed with brine, dried over anhydrous $Na_2SO_4$, and evaporated under reduced pressure. The product was purified by silica gel column chromatography ($CH_2Cl_2$ : MeOH = 95 : 5) to give **4** (823 mg, 84.7%). $^1$H NMR (400 MHz, DMSO-$d_6$) $\delta$ 7.41 (t, $J$ = 5.6 Hz, 1H), 7.29 (t, $J$ = 5.9 Hz, 1H), 6.63–6.59 (m, 1H), 5.93 (s, 1H), 2.92 (dd, $J$ = 13.7, 6.2 Hz, 1H), 2.65 (t, $J$ = 7.0 Hz, 1H); $^{13}$C NMR (101 MHz, DMSO-$d_6$) $\delta$ 152.6, 128.5, 125.2, 112.7, 41.8, 37.0. HRMS (ESI): $m/z$ [M + H]$^+$ calculated for $C_{16}H_{23}N_4O_4S_4^+$: 463.0597; found: 463.0597.

**4** (523 mg, 1.1 mmol) was dissolved in 20 mL concentrated HCl and 20 mL $H_2O$ and cooled down to 0 °C. The water solution of $NaNO_2$ (483 mg, 7.0 mmol) was slowly added to the mixture at 0 °C. After reaction for 1 h, 2 mL 60% $HPF_6$ was added and the mixture was stirred for 1 h. The product was collected by filtration and washed with ice-cold water, yielding a yellow solid of **DDA-4** (741 mg, 86.3%). $^1$H NMR (400 MHz, DMSO-$d_6$) $\delta$ 8.87 (d, 4H), 8.60 (t, $J$ = 5.6 Hz, 2H), 8.33 (d, 4H), 3.16 (dd, $J$ = 12.6, 6.4 Hz, 4H), 2.75 (t, $J$ = 6.7 Hz, 4H); $^{13}$C NMR (101 MHz, DMSO-$d_6$) $\delta$ 150.3, 134.1, 128.7, 120.0, 41.7, 37.1; $^{31}$P NMR (162 MHz, DMSO-$d_6$) $\delta$ −144.19 (h, $J_{P\text{-}F}$ = 711.3 Hz).

### UV-Vis spectrophotometry assay

All spectroscopic measurements were performed in phosphate-buffered saline buffer (50 mM, pH 7.4, containing 5% DMSO) in a 3 mL corvette with 2 mL solution. Compounds were dissolved into DMSO to prepare the stock solutions with a concentration of 200 mM Tyr or 20 mM diazonium reagent.

Reaction of the diazonium reagent (**DDA-2** or **DDA-3**) and Tyr-containing molecule (H-Tyr-OBzl Tos): 2 μL **DDA-2** or **DDA-3**

 

and 4 μL Tyr was added to 1994 μL buffer. The progress of the reaction was monitored by UV-Vis spectrophotometry from 250 to 600 nm.

Determination of the kinetic parameters of the reaction between the diazonium reagent (**DDA-2** or **DDA-3**) and tyrosine: the reaction rate was measured under pseudo-first order conditions, where 20 μM **DDA-2** or **DDA-3** was mixed with an excess of tyrosine (0.1–1 mM) in PBS buffer (50 mM, pH 7.4, containing 5% DMSO) and the absorption at 400 nm was recorded per second.

### TMV and TMV CP purification

According to our previous procedure, TMV virus and TMV capsid proteins were purified.[12a]

TMV purification: TMV-inoculated tobacco leaves were ground fully and mixed in 25 mL 0.2 M phosphate buffer (pH 7.0) including 250 μL β-mercaptoethanol (1%, v/v) on ice. After the filtration with two-layer screen cloth, the clear lysates were mixed with *n*-butyl alcohol (8%, v/v) for 15 min. After centrifugation at 10 000 × *g* for 20 min, the precipitate was dissolved again with 2 mL 0.01 M phosphate buffer (pH 7.0) on ice and stirred for 6 h. After centrifugation at 10 000 × *g* for 20 min, the pellet was resuspended in 5 mL 0.01 M phosphate buffer (pH 7.0) for 2 h. After centrifugation at 10 000 × *g* for 20 min, the supernatant was then added with NaCl (4%, w/v) and PEG6000 (4%, w/v) for overnight precipitation. After centrifugation at 10 000 × *g* for 20 min, the precipitate was resuspended in 2 mL 0.01 M phosphate buffer (pH 7.0) for 6 h. After centrifugation at 10 000 × *g* for 5 min, the final virus suspension was obtained and the virus purity was evaluated according to the indicated ratio of $A_{280}/A_{260}$ (0.84) and $A_{260}/A_{248}$ (1.09). TMV concentration was calculated according to C (mg mL$^{-1}$) = $A_{260}$/3.1. TMV solution was stored at 4 °C for the following test.

Purification of TMV capsid proteins (TMV CP): TMV solution was firstly diluted to 5 mg mL$^{-1}$ and then stirred with two volumes of glacial acetic acid for 2 h at 4 °C. Subsequently, an equal volume of sterile water was added and all the liquid was then transferred into the dialysis bag. After three to five times of water exchange, TMV CP precipitated. After centrifugation at 12 000 rpm for 30 min, TMV CP precipitate was obtained and dissolved in 50 μL 0.1 M phosphate buffer (pH 7.0). The concentration of TMV CP was calculated according to C (mg mL$^{-1}$) = $A_{282}$/1.27. TMV CP was stored at 4 °C for the following test.

### Crosslinking TMV CP and TMV virus with the dual-diazonium reagent

TMV CP crosslinking: TMV CP crosslinking was performed by mixing TMV CP with various concentrations of the dual-diazonium reagent (**DDA-1**, **DDA-2**, **DDA-3**). The dual-diazonium reagent was diluted to a gradient concentration (100, 50, 25, 12.5, 6.25, 3.12, 1.56, mM). The reaction was performed by mixing 9 μL TMV CP (2 μg μL$^{-1}$) and 1 μL the dual-diazonium reagent (100, 50, 25, 12.5, 6.25, 3.12, 1.56, mM). The reaction was incubated at 25 °C for 30 min.

TMV virus crosslinking: TMV virus crosslinking was performed by mixing TMV virus with various concentrations of the dual-diazonium reagent (**DDA-1**, **DDA-2**, **DDA-3**). The dual-diazonium reagent was diluted to a gradient concentration (100, 50, 25, 12.5, 6.25, 3.12, 1.56, mM). The reaction was performed by mixing 9 μL TMV virus (1 μg μL$^{-1}$) and 1 μL the dual-diazonium reagent (100, 50, 25, 12.5, 6.25, 3.12, 1.56, mM). The reaction was incubated at 25 °C or 37 °C for 30 min or 60 min.

After reaction, all samples were mixed with 5× SDS loading buffer and used for 12% SDS-PAGE assay. The SDS-PAGE gel was stained with Coomassie blue R250 and imaged with Quantity One software (Bio-Rad).

### Construction of TMV hydrogel with the dual-diazonium reagent

To optimize conditions for hydrogel preparation, we tried different concentrations of TMV matrix (0–10 mg mL$^{-1}$) and **DDA-3** (0–10 mM). TMV hydrogel was made by gently mixing different concentrations of **DDA-3** and TMV solution in a glass vial at room temperature for 0–30 min to evaluate the gelation condition.

For TMV hydrogel with 2.5 mg mL$^{-1}$ TMV matrix and 10 mM **DDA-2 or DDA-3**, **DDA-2 or DDA-3** was freshly prepared in DMSO as 100 mM stock solution. 50 μL of **DDA-2 or DDA-3** (100 mM) was added to 325 μL of 0.1 M phosphate buffer (pH 7.0) to prepare solution A; 62.5 μL of TMV solution (20 mg mL$^{-1}$) was added to 62.5 μL of phosphate buffer to prepare solution B. The reaction was performed by mixing solution A and solution B. The gelation of TMV hydrogel was observed within 30 min at room temperature. It was the same for **DDA-4** constructed hydrogel except that the concentration of **DDA-4** and TMV matrix were 2 mM and 2.5 mg mL$^{-1}$, respectively.

### Scanning electron microscopy (SEM) characterization

TMV hydrogel was made by 5 mg mL$^{-1}$ TMV and 10 mM **DDA-2** or **DDA-3** at room temperature for 1 h. Then, the hydrogel was firstly cold-dried and loaded onto the sample vessel. The sample was imaged using a Hitachi S-4700 field emission SEM.

### Rheology

All rheological measurements were performed using an ar2000ex Rheometer from TA Instruments at 25 °C. When the crosslinking reagent and the TMV solution were mixed, the mixture was quickly added to the mold to start testing before the hydrogel was completely solidified. TMV hydrogel was made by 2.5 mg mL$^{-1}$ TMV and 10 mM **DDA-2** or **DDA-3**. Due to the faster rate of **DDA-3** crosslinking, we formulated this hydrogel in ice-water bath conditions.

### TMV hydrogel degradation

To degrade virus hydrogel with chemical agents, TMV hydrogel was made according to the above procedure with **DDA-4**. The TMV hydrogel was degraded by dithiothreitol (DTT). We firstly carved the word "BUCT" and "NKU" on the Petri dish. The hydrogel was made by transferring the mixture of 2.5 mg mL$^{-1}$

TMV and 2 mM **DDA-4** on the word groove for gelation at room temperature. After gelation, 20 mL DTT (500 mM) as the test group and 20 mL deionized water as the control group were transferred into the Petri dish to immerse the TMV hydrogel. The gel degradation was imaged at different time (0–12 h).

## Conflicts of interest

There are no conflicts to declare.

## Acknowledgements

This work was supported by NSFC (21572019) and Beijing Municipal Natural Science Foundation (2192038).

## Notes and references

1 (*a*) S. R. Caliari and J. A. Burdick, *Nat. Methods*, 2016, **13**, 405–414; (*b*) K. T. Dicker, J. Song, A. C. Moore, H. Zhang, Y. Li, D. L. Burris, X. Jia and J. M. Fox, *Chem. Sci.*, 2018, **9**, 5394–5404; (*c*) O. Chaudhuri, *Biomater. Sci.*, 2017, **5**, 1480–1490; (*d*) S. J. Kim, J. Park, H. Byun, Y. W. Park, L. G. Major, D. Y. Lee, Y. S. Choi and H. Shin, *Biomaterials*, 2019, **188**, 198–212; (*e*) M. W. Tibbitt and K. S. Anseth, *Biotechnol. Bioeng.*, 2009, **103**, 655–663; (*f*) T. Bai, A. Sinclair, F. Sun, P. Jain, H.-C. Hung, P. Zhang, J.-R. Ella-Menye, W. Liu and S. Jiang, *Chem. Sci.*, 2016, **7**, 333–338.

2 (*a*) J. Xing, M. Zheng and X. Duan, *Chem. Soc. Rev.*, 2015, **44**, 5031–5039; (*b*) X. Mao, G. Chen, Z. Wang, Y. Zhang, X. Zhu and G. Li, *Chem. Sci.*, 2018, **9**, 811–818; (*c*) B. Balakrishnan and R. Banerjee, *Chem. Rev.*, 2011, **111**, 4453–4474; (*d*) S. Reakasame and A. R. Boccaccini, *Biomacromolecules*, 2018, **19**, 3–21; (*e*) M. Mehrali, A. Thakur, C. P. Pennisi, S. Talebian, A. Arpanaei, M. Nikkhah and A. Dolatshahi-Pirouz, *Adv. Mater.*, 2017, **29**, 1603612; (*f*) A. Brito, Y. M. Abul-Haija, D. S. da Costa, R. Novoa-Carballal, R. L. Reis, R. V. Ulijn, R. A. Pires and I. Pashkuleva, *Chem. Sci.*, 2019, **10**, 2385–2390; (*g*) Y. P. Singh, J. C. Moses, N. Bhardwaj and B. B. Madal, *J. Mater. Chem. B*, 2018, **6**, 5499–5529.

3 (*a*) S. Merino, C. Martin, K. Kostarelos, M. Prato and E. Vazquez, *ACS Nano*, 2015, **9**, 4686–4697; (*b*) J. Tsai, T. Zou, J. Liu, T. Chen, A. Chan, C. Yang, C. Lok and C. Che, *Chem. Sci.*, 2015, **6**, 3823–3830; (*c*) J. Xing, M. Zheng and X. Duan, *Chem. Soc. Rev.*, 2015, **44**, 5031–5039; (*d*) M. R. Saboktakin and R. M. Tabatabaei, *Int. J. Biol. Macromol.*, 2015, **75**, 426–436; (*e*) R. Dimatteo, N. J. Darling and T. Segura, *Adv. Drug Delivery Rev.*, 2018, **127**, 167–184; (*f*) T. Su, Z. Tang, H. He, W. Li, X. Wang, C. Liao, Y. Sun and Q. Wang, *Chem. Sci.*, 2014, **5**, 4204–4209; (*g*) B. D. Monnery and R. Hoogenboom, *Polym. Chem.*, 2019, **10**, 3480–3487.

4 (*a*) D. Stern and H. Cui, *Adv. Healthcare Mater.*, 2019, **8**, e1900104; (*b*) G. M. Guebitz and G. S. Nyanhongo, *Trends Biotechnol.*, 2018, **36**, 1040–1053; (*c*) Q. Xu, L. Guo, A. Sigen, Y. Gao, D. Zhou, U. Greiser, J. Creagh-Flynn, H. Zhang, Y. Dong, L. Cutlar, F. Wang, W. Liu, W. Wang and W. Wang, *Chem. Sci.*, 2018, **9**, 2179–2187; (*d*) A. H. Morris, H. Lee, H. Xing, D. K. Stamer, M. Tan and T. R. Kyriakides, *ACS Appl. Mater. Interfaces*, 2018, **10**, 41892–41901; (*e*) X. Chen, Z. Yue, P. C. Winberg, J. N. Dinoro, P. Hayes, S. Beirne and G. G. Wallace, *Biomater. Sci.*, 2019, **10**, 41892–41901; (*f*) S. An, E. J. Jeon, J. Jeon and S. Cho, *Mater. Horiz.*, 2019, **6**, 1169–1178; (*g*) H. Jiang, M. Ochoa, J. F. Waimin, R. Rahimi and B. Ziaie, *Lab Chip*, 2019, **19**, 2265–2274.

5 (*a*) E. M. Ahmed, *J. Adv. Res.*, 2015, **6**, 105–121; (*b*) H. Yuk, B. Lu and X. Zhao, *Chem. Soc. Rev.*, 2019, **48**, 1642–1667; (*c*) X. Le, W. Lu, J. Zheng, D. Tong, N. Zhao, C. Ma, H. Xiao, J. Zhang, Y. Huang and T. Chen, *Chem. Sci.*, 2016, **7**, 6715–6720; (*d*) T. E. Brown and K. S. Anseth, *Chem. Soc. Rev.*, 2017, **46**, 6532–6552; (*e*) S. An, E. J. Jeon, J. Jeon and S. Cho, *Mater. Horiz.*, 2019, **6**, 1169–1178.

6 (*a*) Y. Zhu, Q. Zhang, X. Shi and D. Han, *Adv. Mater.*, 2019, e1804950; (*b*) C. Chen, L. Wang, L. Deng, R. Hu and A. Dong, *J. Biomed. Mater. Res., Part A*, 2013, **101**, 684–693; (*c*) S. De Koker, J. Cui, N. Vanparijs, L. Albertazzi, J. Grooten, F. Caruso and B. G. De Geest, *Angew. Chem., Int. Ed.*, 2016, **55**, 1334–1339; (*d*) C. Wang, M. Fadeev, J. Zhang, M. Vázquez-González, G. Davidson-Rozenfeld, H. Tian and I. Willner, *Chem. Sci.*, 2018, **9**, 7145–7152; (*e*) Y. Wang, Y. Li, X. Yu, Q. Long and T. Zhang, *RSC Adv.*, 2019, **9**, 18394–18405; (*f*) J. Du, S. Xu, S. Feng, L. Yu, J. Wang and Y. Liu, *Soft Matter*, 2016, **12**, 1649–1654.

7 (*a*) A. M. Wen and N. F. Steinmetz, *Chem. Soc. Rev.*, 2016, **45**, 4074–4126; (*b*) T. L. Schlick, Z. Ding, E. W. Kovacs and M. B. Francis, *J. Am. Chem. Soc.*, 2005, **127**, 3718–3723; (*c*) K. Mohan and G. A. Weiss, *ACS Chem. Biol.*, 2016, **11**, 1167–1179; (*d*) Z. Liu, J. Qiao, Z. Niu and Q. Wang, *Chem. Soc. Rev.*, 2012, **41**, 6178–6194; (*e*) R. Farr, D. S. Choi and S. W. Lee, *Acta Biomater.*, 2014, **10**, 1741–1750; (*f*) M. A. Bruckman, G. Kaur, L. A. Lee, F. Xie, J. Sepulveda, R. Breitenkamp, X. Zhang, M. Joralemon, T. P. Russell, T. Emrick and Q. Wang, *ChemBioChem*, 2008, **9**, 519–523.

8 (*a*) S. Honarbakhsh, R. H. Guenther, J. A. Willoughby, S. A. Lommel and B. Pourdeyhimi, *Adv. Healthcare Mater.*, 2013, **2**, 1001–1007; (*b*) K. L. Kozielski, Y. Rui and J. J. Green, *Expert Opin. Drug Delivery*, 2016, **13**, 1475–1487; (*c*) M. Wu, J. Shi, D. Fan, Q. Zhou, F. Wang, Z. Niu and Y. Huang, *Biomacromolecules*, 2013, **14**, 4032–4037; (*d*) N. M. Gulati, A. S. Pitek, A. E. Czapar, P. L. Stewart and N. F. Steinmetz, *J. Mater. Chem. B*, 2018, **6**, 2204–2216; (*e*) P. Lam, R. D. Lin and N. F. Steinmetz, *J. Mater. Chem. B*, 2018, **6**, 5888–5895; (*f*) A. S. Pitek, J. Park, Y. Wang, H. Gao, H. Hu, D. I. Simon and N. F. Steinmetz, *Nanoscale*, 2018, **10**, 16547–16555.

9 (*a*) N. F. Steinmetz and D. J. Evans, *Org. Biomol. Chem.*, 2007, **5**, 2891–2902; (*b*) B. D. B. Tiu, D. L. Kernan, S. B. Tiu, A. M. Wen, Y. Zheng, J. K. Pokorski, R. C. Advincula and N. F. Steinmetz, *Nanoscale*, 2017, **9**, 1580–1590.

10 (*a*) J. A. Luckanagul, L. A. Lee, S. J. You, X. M. Yang and Q. Wang, *J. Biomed. Mater. Res., Part A*, 2015, **103**, 887–895; (*b*) A. Southan, T. Lang, M. Schweikert, G. E. M. Tovar, C. Wege and S. Eiben, *RSC Adv.*, 2018, **8**, 4686–4694; (*c*)

 

L. Chen, X. Zhao, Y. Lin, Z. Su and Q. Wang, *Polym. Chem.*, 2014, **5**, 6754–6760; (*d*) X. Liu, J. Zhang, M. Fadeev, Z. Li, V. Wulf, H. Tian and I. Willner, *Chem. Sci.*, 2019, **10**, 1008–1016.

11 D. Ma, J. Zhang, C. Zhang, Y. Men, H. Sun, L. Li, L. Yi and Z. Xi, *Org. Biomol. Chem.*, 2018, **16**, 3353–3357.

12 (*a*) D. Ma, Y. Xie, J. Zhang, D. Ouyang, L. Yi and Z. Xi, *Chem. Commun.*, 2014, **50**, 15581; (*b*) J. Zhang, D. Ma, D. Du, Z. Xi and L. Yi, *Org. Biomol. Chem.*, 2014, **12**, 9528; (*c*) J. Zhang, Y. Men, S. Lv, L. Yi and J. Chen, *Org. Biomol. Chem.*, 2015, **13**, 11422; (*d*) D. Ma, X. Kang, Y. Gao, J. Zhu, L. Yi and Z. Xi, *Tetrahedron*, 2019, **75**, 888–893.

13 (*a*) Y. Heider, N. E. Poitiers, P. Willmes, K. I. Leszczynska, V. Huch and D. Scheschkewitz, *Chem. Sci.*, 2019, **10**, 4523–4530; (*b*) L. P. Hammett, *Chem. Rev.*, 1935, **17**, 125–136; (*c*) L. P. Hammett, *J. Am. Chem. Soc.*, 1937, **59**, 96–103.

14 C. Hansch, A. Leo and R. W. Taft, *Chem. Rev.*, 1991, **91**, 165–195.

15 (*a*) J. R. Fores, M. Criado-Gonzalez, M. Schmutz, C. Blanck, P. Schaaf, F. Boulmedais and L. Jierry, *Chem. Sci.*, 2019, **10**, 4761–4766; (*b*) H. G. Li, D. Buesen, R. Williams, J. Henig, S. Stapf, K. Mukherjee, E. Freier, W. Lubitz, M. Winkler, T. Happee and N. Plumeré, *Chem. Sci.*, 2018, **9**, 7596–7605.